Published in final edited form as:
*Nat Nanotechnol*. 2017 December ; 12(12): 1190–1198. doi:10.1038/nnano.2017.188.

# A synthetic intrabody based selective and generic inhibitor of GPCR endocytosis

**Eshan Ghosh**[1], **Ashish Srivastava**[1], **Mithu Baidya**[1], **Punita Kumari**[1], **Hemlata Dwivedi**[1], **Kumari Nidhi**[1], **Ravi Ranjan**[1], **Shalini Dogra**[2], **Akiko Koide**[3,4], **Prem N. Yadav**[2], **Sachdev S. Sidhu**[5], **Shohei Koide**[3,6], and **Arun K. Shukla**[1,*]

[1]Department of Biological Sciences and Bioengineering, Indian Institute of Technology, Kanpur 208016, India

[2]CSIR-Central Drug Research Institute, Lucknow, India

[3]Laura and Isaac Perlmutter Cancer Center, New York University Langone Medical Center, New York, NY 10016, USA

[4]Department of Medicine, New York University School of Medicine, New York, NY 10016, USA

[5]Department of Molecular Genetics, University of Toronto, Ontario MSS1A8, Canada

[6]Department of Biochemistry and Molecular Pharmacology, New York University School of Medicine, New York, NY 10016, USA

## Abstract

β-arrestins (βarrs) critically mediate desensitization, endocytosis and signaling of G Protein-Coupled Receptors (GPCRs), and they scaffold a large number of interaction partners. However, allosteric modulation of their scaffolding abilities and direct targeting of their interaction interfaces to selectively modulate GPCR functions have not been fully explored yet. Here, we have identified a series of synthetic antibody fragments (Fabs) against different conformations of βarrs from phage display libraries. Several of these Fabs allosterically and selectively modulated the



*Correspondence and requests for materials should be addressed to AKS.

**Author Contributions**

EG designed, optimized and performed the endocytosis and ERK activation experiments with ScFv5 intrabody, cross-linking experiment with ScFv5 and assisted in ERK assays; AS performed ELISA based assessment of clathrin and ERK interaction with βarr, assisted in endocytosis and ERK assays; MB performed the confocal microscopy using ScFv5-YFP intrabody and assisted in sub-cloning and endocytosis experiments; PK carried out ELISA based selectivity test for βarr2 Fabs, carried out endocytosis and ERK assays for $M_2R$ and $\beta_2V_2R$ together with MB; HD carried out the selectivity assays for Fabs by coIP together with AS, ELISA based selectivity assay for Fab5 and ScFv5, and mapping experiment for ScFv5; RR converted the Fabs into intrabodies for expression, assisted in sub-cloning of various constructs and endocytosis experiments; KN performed the initial phase of intrabody expression, functional validation and their effect on receptor endocytosis and ERK activation; SD and PNY assisted in the βarr knock-down; SSK, AK and SS provided the phage display libraries; AKS carried out the phage display screening, wrote the manuscript, and supervised the overall project design and execution. All authors approved the final draft of the manuscript.

**Data Availability Statement**

The data that support the plots within this paper and other findings of this study are available from the corresponding author upon reasonable request.

**Competing Financial Interest**

The authors declare no competing financial interest.


Europe PMC Funders Author Manuscripts

interaction of βarrs with clathrin and ERK MAP kinase. Interestingly, one of these Fabs selectively disrupted βarr-clathrin interaction, and when expressed as an intrabody, it robustly inhibited agonist-induced endocytosis of a broad set of GPCRs without affecting ERK MAP kinase activation. Our data therefore demonstrate the feasibility of selectively targeting βarr interactions using intrabodies and provide a novel framework for fine-tuning GPCR functions with potential therapeutic implications.

**Keywords**

GPCRs; β-arrestins; cellular signaling; endocytosis; ERK MAP kinase; Phage Display; synthetic antibody fragments; intrabodies

Signaling and regulation of the G Protein-Coupled Receptors (GPCRs), also known as the seven transmembrane receptors (7TMRs), are critically regulated by β-arrestins (βarrs)1. Majority of βarr functions in the context of GPCR regulation and signaling are mediated primarily by their scaffolding abilities of various interaction partners2,3. For example, βarrs scaffold clathrin heavy chain and β2 adaptin subunit of the AP2 complex to promote agonist-induced GPCR endocytosis4,5. Similarly, βarrs nucleate various components of MAP kinase cascade to facilitate G protein independent signaling3,6,7. Conventionally, siRNA and gene knock-out approaches have been used to dissect specific contributions of βarrs in GPCR functions8,9. However, it remains unexplored whether selective βarr functions can be targeted with biochemical tools that allosterically modulate their scaffolding abilities or directly target their interaction interfaces. Unlike suppression of all βarr functions by gene knock-down or knock-out approaches that deplete the entire protein, selective targeting of βarr functions is likely to offer a unique handle on dissecting the fine modalities of GPCR-βarr signaling axis. Biochemical studies have revealed that βarrs scaffold many of their interaction partners through non-overlapping interaction interfaces (Fig. 1a)10–18. Therefore, we envisioned that targeted disruption of selective interaction interfaces or allosteric modulation of specific βarr interactions can be leveraged to influence specific βarr-dependent GPCR functions. Accordingly, we set out to generate and evaluate antibody fragments targeting different conformations and binding interfaces of βarrs to modulate two major βarr interactions namely, clathrin and ERK2, and corresponding functional outcomes i.e. agonist-induced GPCR endocytosis and ERK MAP kinase activation.

## Fab30 selectively enhances βarr1-ERK2 interaction

We first tested a previously described antibody fragment, referred to as Fab30, that selectively recognizes and stabilizes an active βarr1 conformation induced by the binding of a phosphorylated peptide (referred to as $V_2$Rpp) corresponding to the carboxyl terminus of the human vasopressin receptor ($V_2$R)19. As the epitope of Fab30 does not directly overlap with clathrin or ERK2 binding regions on βarr1, we reasoned that it may be a good candidate to evaluate as an allosteric modulator of βarr1 interactions with clathrin and ERK2. We first confirmed the selectivity of Fab30 for $V_2$Rpp-bound βarr1 conformation (Fig. 1b), and then tested its effect on βarr1-ERK2/clathrin interactions. The interaction of




Europe PMC Funders Author Manuscripts

βarrs with clathrin is substantially enhanced by the presence of $V_2$Rpp while their interaction with ERK2 does not change significantly by $V_2$Rpp20–22. Therefore, to maintain similar experimental conditions, we used $V_2$Rpp-bound βarr1 in this experiment as well as in subsequent experiments measuring the effect of Fabs on different βarr interactions. As presented in Fig. 1c and Supplementary Fig. 1, pre-incubation of βarr1 with Fab30 resulted in a significant potentiation of βarr1-ERK2 interaction while a control Fab (Fab-CTL) that does not interact with βarr1 had no significant effect. Furthermore, Fab30 also exhibited similar potentiation of βarr1-pERK2 (active ERK2) interaction (Fig. 1d). Interestingly however, Fab30 did not alter the interaction between βarr1 and clathrin in the same experimental set-up (Fig. 1e). These findings provide the proof-of-principle evidence suggesting that allosteric modulation of selective βarr interactions is possible by antibody fragments targeting βarrs.

## Fab5 selectively disrupts βarr2-clathrin interaction

Inspired by these observations, we set out to select additional Fabs targeting βarrs in an attempt to identify additional modulators of βarr interactions. There are two isoforms of βarrs (βarr1 and 2; also referred to as arrestin 2 and 3, respectively) that have overall very similar three-dimensional structures23,24. βarr1 and 2 share many functions although recent studies have also identified a significant functional divergence of the two isoforms in the context of GPCR signaling and regulation25. We used a previously described phage display library26 of Fabs to select specific binders against βarr1 and 2 following previously published protocols27,28 (Fig. 2a). In addition to those binding to βarr1 and 2, we also selected Fabs against $V_2$Rpp-βarr1-Fab30 complex in order to isolate additional Fabs that can recognize active βarr1 conformation and bind to a βarr1 interface that is distinct from that of Fab30. A list of different Fabs generated and characterized in this study is presented in the Supplementary Table 1.

From the set of new Fabs selected against $V_2$Rpp-βarr1-Fab30 complex, we observed that several Fabs specifically recognized $V_2$Rpp-bound βarr1 conformation, similar to Fab30 (Fig. 2b, left panel and Supplementary Fig. 2a). One of these Fabs, referred to as Fab12, significantly potentiated both, βarr1-clathrin and βarr1-ERK2 interactions (Fig. 2b, right panel and Supplementary Fig. 2b). From the set of Fabs selected against βarr1, two of them selectively recognized βarr1 over βarr2 (Fig. 2c, left panel and Supplementary Fig. 3a). One of these Fabs, referred to as Fab9, robustly potentiated βarr1-ERK2 interaction without affecting βarr1-clathrin binding (Fig. 2c, right panel). Finally, our phage display selection on βarr2 also yielded several Fabs that displayed striking selectivity for βarr2 over βarr1 (Fig. 2d and Supplementary Fig. 4a-e. Most interestingly, one of these Fabs, referred to as Fab5, robustly inhibited βarr2-clathrin interaction (Fig. 2e) without significantly affecting the binding of βarr2 with ERK2 or phophso-ERK2 (Fig. 2f). These findings with Fab5 demonstrate the feasibility of selectively inhibiting specific βarr interactions with antibody fragments. It also raises the possibility that Fab5, as an intrabody, might be an inhibitor of the endocytosis of those GPCRs that utilize βarr-clathrin interaction as a key driving force for their internalization. Therefore, we focused on investigating the effect of Fab5 based intrabody on agonist-induced GPCR internalization.

## Fab5 maintains its functionality as an intrabody

Cytoplasmic milieu of mammalian cells is reducing in nature while functional assembly of Fabs requires the formation of disulphide bonds. Therefore, we decided to express the single chain version of Fab5, referred to as ScFv5, as an intrabody in cellular context for evaluating its effect on GPCR endocytosis. Before that, we tested and confirmed the ability of ScFv5 to maintain its binding and selectivity for βarr2 (Fig. 3a-b, Supplementary Fig. 6a), and its ability to specifically inhibit βarr2-clathrin interaction, similar to Fab5 (Fig. 3c). To further confirm the selectivity of ScFv5 for βarr2-clathrin interaction, we also measured its effect on βarr2-β2 adaptin and βarr2-JNK3 interactions. We observed that ScFv5 had a small inhibitory effect on the βarr2-β2 adaptin and βarr2-JNK3 interactions at higher concentrations but it was not as robust as its effect on the βarr2-clathrin interaction (Supplementary Fig. 5).

Furthermore, in order to gain a mechanistic insight into the ability of ScFv5 to inhibit βarr2-clathrin interaction, we mapped its interaction interface on βarr2 using a series of truncated βarr2 constructs. We observed that the distal carboxyl terminus of βarr2 was a key binding site for ScFv5 but the N-domain of βarr2 was also required for binding (Fig. 3d). As the clathrin binding interface is localized primarily to the distal carboxyl terminus of βarrs29, this observation suggests that the inhibition of βarr2-clathrin interaction by ScFv5 is likely to be due primarily to a direct competition between ScFv5 and clathrin for a binding interface on βarr2. Nevertheless, the requirement of the N-domain of βarr2, which is away from the clathrin binding site, also suggests that ScFv5 mediated inhibition of βarr2-clathrin interaction is, at least in part, regulated in allosteric fashion as well.

In order to validate the functionality of ScFv5 as an intrabody, we expressed it in HEK-293 cells as HA-tagged and YFP-tagged constructs. We measured the ability of ScFv5 intrabody to immunoprecipitate βarr2 and its overall cellular distribution. We observed that ScFv5 as an intrabody robustly immunoprecipitated βarr2 (Fig. 3e) which confirms its functionality. We also found that that ScFv5-YFP was evenly distributed in the cytoplasm, very similar to the basal distribution of βarr2-mCherry (Supplementary Fig. 6b).

## Intrabody 5 selectively inhibits $V_2R$ endocytosis

In order to evaluate the effect of ScFv5 intrabody on GPCR endocytosis, we first used the human vasopressin receptor ($V_2R$) as a prototypical GPCR. A prerequisite for ScFv5 intrabody to potentially inhibit GPCR endocytosis would be that it should not interfere with receptor-βarr2 interaction. Therefore, we first tested agonist-dependent interaction of $V_2R$ and βarr2 in the presence of ScFv5. We observed that in HEK-293 cells expressing $V_2R$, βarr2-mCherry and ScFv5 (as intrabody), βarr2-mCherry was recruited to the plasma membrane upon agonist stimulation (within 2-5 min) (Fig. 3f), and interestingly, ScFv5 was also colocalized with βarr2 at the plasma membrane (Fig. 3f). We also carried out a coimmunoprecipitation experiment which also revealed that ScFv5 did not affect βarr2 interaction with $V_2R$ upon agonist stimulation (Fig. 3g). Moreover, we also observed that ScFv5 exhibited robust interaction with $V_2R$pp-bound βarr2, at slightly higher levels than basal conformation of βarr2, further confirming its ability to recognize activated βarr2

conformation (Supplementary Fig. 7). Under basal condition, the carboxyl terminus of βarrs is tethered in the N-domain through a set of specific interactions, and binding of GPCRs results in the release of the carboxyl terminus. This exposes the primary clathrin binding site located in the carboxyl terminus of βarrs resulting in binding of clathrin and subsequent receptor internalization. The enhancement in the interaction of ScFv5 with βarr2 in the presence of $V_2$Rpp suggests that the release of carboxyl terminus is not only compatible but also favorable for ScFv5 binding. This also explains how ScFv5 as an intrabody is able to occupy receptor-bound βarr2 and thereby preclude the interaction of clathrin resulting in the inhibition of receptor endocytosis. Taken together, these data establish that ScFv5 does not interfere with $V_2$R-βarr2 interaction and it can interact with receptor-bound βarr2 conformation.

Next, we measured agonist-induced $V_2$R endocytosis in HEK-293 cells expressing ScFv5 as an intrabody. As presented in Fig. 4a, we observed a robust inhibition of $V_2$R endocytosis by ScFv5 intrabody which is in line with its ability to inhibit βarr2-clathrin interaction. To further corroborate this finding and to directly visualize the effect of ScFv5 intrabody on $V_2$R internalization, we next utilized the confocal microscopy approach. GPCRs can be categorized into two distinct subclasses referred to as class A and B with respect to βarr recruitment pattern30. While class A GPCRs such as $\beta_2$ adrenergic receptor ($\beta_2$AR) exhibit a transient interaction with βarrs and rapid recycling, class B GPCRs such as $V_2$R display prolonged interaction with βarrs and endosomal co-localization with βarrs after agonist stimulation. As presented in Fig. 4b (upper panel), confocal microscopy of cells expressing ScFv-CTL as intrabody revealed that βarr2-mCherry was recruited to the membrane at early time points of agonist stimulation (90-180 sec) and subsequently, after prolonged agonist exposure (600-1800 sec), it was localized to endosomal vesicles. Interestingly, in ScFv5 intrabody-expressing cells, βarr2-mCherry was targeted to the plasma membrane at early time points as anticipated, but the formation of endosomal vesicles was significantly attenuated (Fig. 4b, lower panel and Fig. 4c). In these cells, βarr2-mCherry remained localized at the plasma membrane together with ScFv5 (Supplementary Fig. 8). To further confirm these findings, we imaged multiple cells (>100) at multiple Z-positions to cover the entire volume of the cells and quantified the puncta (i.e. endosomal vesicles representing internalized receptors) from ScFv-CTL and ScFv5 expressing cells. As presented in Supplementary Fig. 9-12, we observed robust inhibition of agonist-induced $V_2$R internalization at all three time points that were tested. In some cells, we did observe the formation of a few βarr2 containing endosomal vesicles, however, they did not display colocalization with ScFv5 (Supplementary Fig. 13). This most likely arises either from a small population of βarr2 that escapes interaction with ScFv5 or due to the contribution of βarr1 in the endocytosis of $V_2$R.

## Intrabody 5 does not affect ERK MAP kinase activation

In addition to endocytosis, βarrs can also mediate G protein independent ERK activation downstream of GPCRs. Therefore, we measured the effct of ScFv5 intrabody on agonist-induced ERK activation downstream of the $V_2$R. Extensive biochemical studies have revealed that ERK activation downstream of GPCRs, including the $V_2$R, is typically biphasic in nature. The first phase (0-5 min post-agonist stimulation) is mostly G protein

dependent while the second phase (10-30 min post-agonist stimulation) is primarily mediated by βarrs3,31. For some receptors however, such as $M_3$ muscarinic receptor and the $H_4$ histamine receptor, the prolonged phase of ERK activation is also mediated by G proteins32,33. We observed that ScFv5 did not affect agonist-induced ERK activation either in the early phase (Fig. 4d) or in the late phase (Fig. 4e). This agrees well with the data presented in Fig. 3c and Fig. 2f that ScFv5/ Fab5 do not inhibit βarr2-ERK binding.

It has been suggested in the literature that the formation of receptor-βarr-ERK signalosomes on internalized vesicles drives the βarr-dependent phase of ERK activation for a number of GPCRs34–36. In other words, endocytosis and βarr-dependent ERK activation are thought to be linked with each other although some receptors do not follow this paradigm 37–40, 56–57. Our data also demonstrate that $V_2R$ endocytosis and ERK activation can indeed be separated from each other, and therefore, it underscores the feasibility of selectively targeting βarr functions in the context of GPCR signaling and regulation using intrabody based approach.

## Intrabody 5 is a generic inhibitor of GPCR endocytosis

The paradigm of βarr mediated clathrin dependent endocytosis is applicable to majority of GPCRs although some receptors exhibit βarr and clathrin independent endocytosis5,41. Therefore, in order to test the generality of ScFv5 intrabody, we measured agonist-induced endocytosis of a broad set of receptors in the presence of ScFv5 intrabody. We observed that similar to $V_2R$, ScFv5 intrabody efficiently inhibited endocytosis of the β2 adrenergic receptor ($\beta_2AR$) (Fig. 5a), the muscarinic receptor subtype 2 ($M_2R$) (Fig. 5b), the dopamine receptor subtypes 1, 2, 3 and 4 ($D_1R$, $D_2R$, $D_3R$ and $D_4R$) (Fig. 5c-f), the μ-opioid receptor (μOR) (Fig. 5g), and a chimeric $\beta_2AR$ harboring the carboxyl terminus of $V_2R$ ($\beta_2V_2R$) (Fig. 5h). Interestingly, similar to $V_2R$, ScFv5 intrabody did not affect ERK activation for these receptors (lower panels in Fig. 5a-f and Supplementary Fig. 14). As expected, ScFv5 intrabody did not influence the agonist-induced internalization of the human muscarinic receptor subtypes 1 and 4 ($M_1R$ and $M_4R$) which undergo βarr independent endocytosis42 (Supplementary Fig. 15). Furthermore, ScFv5 intrabody also did not alter the internalization of the human transferrin receptor 1 (Tfr1) in which undergoes βarr-independent but clathrin-dependent endocytosis (Supplementary Fig. 16 and 17).

As presented in Fig. 5, we notice that ScFv5 inhibited the endocytosis of different receptors to varying extent. This perhaps results from differential dependence of endocytosis on βarr1 vs. 2 for different receptors because ScFv5 exclusively targets βarr2. For example, endocytosis of $\beta_2AR$ is mediated primarily by βarr28 while that of $V_2R$ can be mediated by βarr1 as well43, and this difference leads to more efficient inhibition of $\beta_2AR$ endocytosis compared with $V_2R$ by ScFv5 intrabody. However, we can not rule out the stoichiometric expression levels of βarr2 and ScFv5 intrabody as a contributing factor to this difference. Nevertheless, these findings as a whole reveal that βarr-dependent ERK activation downstream of GPCRs can also be initiated from the plasma membrane without the formation of receptor-βarr-ERK signalosome on endosomal vesicles (Fig. 5i).

## ScFv5 intrabody as a unique tool for modulating GPCR functions

Our approach offers a generic tool to selectively block GPCR endocytosis without affecting ERK activation because it targets an interface on a very well conserved effector (i.e. βarr2) that is distinct from the receptor-effector interaction interface. Previously, two different types of approaches, namely the dominant-negative mutants and the "minigene" constructs, have been used to selectively modulate βarr functions. For example, βarr1$^{V53D}$ and βarr2$^{V54D}$ mutants have been described as dominant-negative for disrupting βarr dependent GPCR endocytosis in numerous studies5,44. Additional βarr mutants (e.g. βarr1$^{\Delta LIELD}$ and βarr1$^{F391A}$) defective in clathrin/adaptin interaction have also been used as dominant-negative for GPCR endocytosis45. A βarr2 mutant, referred to as βarr2$^{KNC}$, which harbors 12 single-point alanine substitutions at key receptor binding residues, acts as a dominant-negative for selectively inhibiting βarr-dependent JNK3 activation46. Along the same lines, βarr1$^{R307A}$ which is deficient in binding c-Raf1 is able to act as a dominant-negative for ERK activation in cells47. Similarly, "minigene" fragments of βarr1 (e.g. residues 319-418) also act as a dominant-negative for receptor endocytosis48. More recently, a "minigene" fragment of βarr1 (residues 25-161) has been utilized elegantly to disrupt the interaction between βarr1 and STAM1 (signal transducing adaptor molecule 1)49,50. βarr1-STAM1 interaction is essential for the auto-phosphorylation and activation of the focal adhesion kinase (FAK), and disrupting the βarr1-STAM1 interaction results in selective attenuation of CXCR4 mediated chemotaxis50. While these constructs are designed by modifying βarrs themselves, RNA aptamers against βarr2, a small molecule AP2 binder, synthetic peptides such as pepducins, and nanobodies targeting the intracellular surface of GPCRs have also been developed to alter some βarr-dependent signaling51–54, 55. Of these, pepducins and receptor-targeting nanobodies remain receptor specific, may not be selective for modulating specific βarr functions and some cases, simply inhibit receptor-βarr interactions.

Although dominant-negative mutants of βarrs are powerful tools for selective inhibition of some specific βarr functions, they might also create an overexpression based gain-of-function effect for other βarr functions. Our intrabody-based approach is not likely to have such a limitation although the extent of strict selectivity of a given intrabody for a specific βarr interaction should be carefully examined. It is important to note that in addition to mediating GPCR endocytosis and ERK MAP kinase activation, βarrs also direct agonist-induced receptor ubiquitination and signaling through other pathways such as JNK, Akt and c-Src3. A comprehensive profiling of entire set of βarr interactions in the presence of ScFv5 in the future should offer interesting insights into the independence and interdependence of various βarr interactions and functions. Furthermore, the conceptual framework applied here can be extended to disrupt other βarr interactions and functions in a selective fashion.

## Conclusions

Taken together, our data establishes that the interactions of βarrs with their partners can be selectively targeted and allosterically modulated using synthetic antibody fragments. Unlike siRNA based conventional approach of gene knockdown that depletes βarrs and hence inhibits all βarr functions downstream of GPCRs, the intrabody based approach offers a unique handle for modulating selected GPCR functions with potential therapeutic

implications. Finally, the ability of ScFv5 intrabody to selectively inhibit endocytosis of many GPCRs provides a novel experimental framework to fine-tune GPCR functions that can be extended not only to other GPCR effectors but likely also to other signaling systems.

## Methods

### General reagents, constructs, cell culture and protein expression

The majority of general chemicals used here for molecular biology, biochemistry and cell biology experiments were purchased from Sigma. Coding regions for different GPCRs described here were obtained from cDNA.org and they were sub-cloned into standard pcDNA3.1 vector with N-terminal signal sequence and a FLAG tag. Purification of Fabs, ScFvs, βarr1 and 2, clathrin and ERK2 were carried out as described previously19. ScFv5-YFP sensor was generated by sub-cloning the ScFv5 coding region in a carboxyl-terminal YFP tag containing pCMV6 based vector for mammalian cell expression. In addition, ScFv5 was also sub-cloned in to pcDNA3.1 vector with carboxyl-terminal HA tag for mammalian cell line expression. Expression plasmids for β2 adaptin, JNK3, TRAF6 and Tfr1 were obtained from Addgene. All constructs were sequence verified (Macrogen) before transfection. DNA transfections were carried out using standard PEI based protocol.

### Phage Display based selection of βarr Fabs

Purified βarr targets were biotinylated using EZ Link Sulpho NHS S-S Biotin (Thermo Pierce), immobilized on Streptavidin Magnetic beads (Promega) and three rounds of screening were carried out as described earlier27. In the third round of selection, phages bound to the immobilized βarr targets were challenged with competitor (i.e. in βarr1 selections, bound phages were challenged with βarr2 while in βarr2 selections, bound phages were challenged with βarr1) to enrich target selective binders. Subsequently, 24 individual clones were tested by phage ELISA on immobilized βarr targets in 96 well MaxiSorp plates. ELISA positive Fab clones were sequenced and a set of unique clones were expressed and purified for further characterization following previously described protocol27.

### Co-immunoprecipitation experiments

In order to evaluate the interaction and selectivity of Fabs (and ScFvs) with βarrs, purified Fabs (1-2μg in 100μL) were incubated with purified βarr1 or 2 (1-2μg in 100μL) for 1h at room temperature (25°C) in binding buffer (20mM Hepes, pH7.4, 100mM NaCl). Subsequently, pre-washed protein L beads were added to the reaction, incubated for additional 1h at room temperature followed by extensive washing (3-5 times in binding buffer + 0.01% Maltose Neopentyl Glycol; MNG) and elution with SDS gel loading buffer. Interaction of Fabs/ScFvs with βarrs was visualized using either Western blotting or SimplyBlue staining of gels.

For mapping the ScFv5 binding interface on βarr2 (Fig. 3d), a series of βarr2 truncation constructs harboring N-terminal GST tag were generated by PCR based cloning, expressed and purified using the same protocol as described earlier for the WT βarr. Equal molar




Europe PMC Funders Author Manuscripts

concentration (1μM) of these constructs were incubated with purified ScFv5 (3-5μM) and their interaction was measured using Protein L beads based coimmunoprecipitation.

In order to validate the functionality of ScFv5 intrabody (Fig. 3e), HA-tagged ScFv5 (in pcDNA3.1 vector) was expressed in HEK-293 cells using PEI based transient transfection. 48h post-transfection, cells were lysed by douncing and incubated with pre-washed HA beads (Sigma). After extensive washing, bound proteins were eluted by SDS gel loading buffer and visualized by Western blotting (βarr antibody – CST – cat. no. 4674, 1:5000; HA antibody –Santa Cruz, cat. no. sc-805, 1:5000).

For measuring the interaction of Fabs to βarrs in cell lysate (Supplementary Fig. 4e), HEK-293 cells expressing βarr1 or βarr2 were first lysed (20mM Hepes, pH7.4, 100mM NaCl, Protease inhibitor cocktail) by douncing and subsequently, the cell lysate was incubated with purified Fabs. After 1h incubation at room temperature with gentle mixing, pre-washed Protein L beads were added to the reaction and incubated further for 1h. Finally, the beads were washed 3-5 times with washing buffer as described above, and eluted proteins were visualized by Western blotting (βarr antibody – CST cat. no. 4674, 1:5000; HRP-coupled Protein L – Genscript cat. no. M00098, 1:2000).

In order to assess the effect of ScFv5 on binding of βarr2 to $V_2R$ (Fig. 3g), *Sf*9 cells expressing $V_2R$ and GRK2 were stimulated with agonist (AVP, 1μM) or inverse agonist (Tolvaptan, 1μM) followed by lysis (20mM Hepes, pH 7.4, 100mM NaCl, Protease and Phosphatase inhibitor cocktail) using glass dounce. Subsequently, βarr2 pre-incubated with indicated ScFv was added to the cell lysate and allowed to bind the receptor for 1h. Freshly prepared DSP (Sigma) (1mM) was added to the reaction mixture and incubated for additional 30 min at room temperature to induce cross-linking of $V_2R$-βarr2 complex. After quenching the reaction with 1M Tris, pH 8.0, pre-washed FLAG M1 antibody beads were added to the mixture and coimmunoprecipitation assay was performed as described above.

### ELISA experiments for measuring Fab-βarr interaction

For single point ELISA (Supplementary Fig. 4a), we first immobilized βarr1 and 2 (1μg in 100μl per well) on a 96 well MaxiSorp plate followed by blocking of potential non-specific binding sites using 1% BSA (Sigma). Subsequently, different Fabs were added (1μg in 100μl per well) to the plate and incubated for 1h at room temperature. Plates were extensively washed (20mM HEPES, pH 7.4, 100mM NaCl and 0.01% MNG) and then the interaction of Fabs with βarrs was visualized by using HRP-coupled Protein L (GenScript, cat. No. M00098, 1:2000 dilution) and TMB ELISA (GenScript). Colorimetric reaction was quenched by adding 1M $H_2SO_4$ and the absorbance was recorded in Victor 4X multimode plate reader (Perkin Elmer) at 450nm. Fab CTL is used as a negative control and it represents a Fab that does not recognize βarrs.

For dose response ELISA experiment (Fig. 2d, Fig.3b and Supplementary Fig. 4b-d), varying concentrations of βarrs were immobilized (as indicated in respective figures) followed by Fab/ScFv (1-2μM) addition and detection using HRP-coupled Protein L as described above.

### Evaluating the effect of Fabs (and ScFvs) on βarr-Clathrin/ERK interaction

For measuring the effect of Fabs (and ScFvs) on βarr interactions, purified clathrin or ERK2 (1-2μg in 100 μL) were immobilized on MaxiSorp ELISA plates followed by blocking of non-specific binding sites with BSA (1% in 200μL per well). Subsequently, biotinylated βarrs (1-3μg in 100μL) pre-incubated with respective Fabs (or ScFv) (varying concentrations as indicated in the figures) were added to individual wells and incubated for 1h at room temperature. After rigorous washing (20mM HEPES, pH 7.4, 100mM NaCl and 0.01% MNG), bound βarrs were visualized using HRP-coupled streptavidin (Genscript cat. no. M00098, 1:5000 dilution) and TMB ELISA (Genscript). Absorbance at 450nm was measured using a multimode plate reader and plotted using GraphPad Prism software. In these experiments, signal in the wells where βarrs were added without any pre-incubation with Fabs (or ScFvs) were used as a normalization reference (treated as 100%). For background correction (i.e. non-specific signal), parallel wells corresponding to every data point without any clathrin or ERK2 were used. As βarr-clathrin interaction is substantially higher in presence of $V_2$Rpp while βarr-ERK2 interaction is about the same in presence or absence of $V_2$Rpp, we have used $V_2$Rpp-bound βarrs in these experiments measuring the effect of Fabs/ScFvs on βarr interactions.

For measuring the effect of Fabs (and ScFvs) on βarr interactions by coimmunoprecipitation (Supplementary Fig. 1 and 2b), purified GST-ERK2 (1-2μg) were first captured on pre-washed GS beads followed by addition of βarrs (pre-incubated with respective Fabs). After 1h incubation at room temperature, beads were washed extensively as described above and bound proteins were eluted using SDS gel loading buffer. Samples were resolved by SDS PAGE and visualized by Western blotting (βarr – CST cat. no. 4674, 1:5000).

### Confocal microscopy

In order to visualize the sub-cellular distribution of ScFv5 and its trafficking to the membrane (Fig. 3f and Supplementary Fig. 13), we transfected 50-60 % confluent 10 cm plate of HEK-293 cells with Flag-$V_2$R, ScFv5 with carboxyl-terminal HA tag and βarr2–mCherry plasmids in 1:1:1 DNA ratio in a total of 7μg DNA mixed with 21 μl polyethylenimine (PEI linear). After 24 hrs, transfected cells were seeded at 1 million cells/well into 6 well plates containing glass cover slips pre-coated with 0.01% poly-D-lysine (Sigma) for 10 mins at RT (room-temperature; 25°C). After another 24h, cells were serum starved for 2 h followed by stimulation with AVP (100 nM) and fixed with 4% formaldehyde (Sigma) diluted in PBS and permeabilized with 0.01% Triton X-100 (Sigma) in PBS for 15-20 min. Subsequently, cells were incubated with rabbit polyclonal anti-HA antibody (cat. no. sc-805 from Santa Cruz Biotechnology; 1:500 dilution) for 1h at RT. After several washes, cells were subsequently incubated with Alexa Fluor 488-conjugated anti-rabbit secondary antibody (A11008, 1:2000, Thermo Fisher Scientific, USA) in 1% BSA for 1h. Cells were subsequently washed three times with PBS followed by incubation with DAPI for nuclear staining (5μg/ml; Sigma) for 5 min at RT. After final washing with PBS, coverslips were mounted on to glass slides using VectaShield H-1,000 mounting medium (VectaShield), allowed to air dry for 15min and then used for confocal microscopy. For the live cell two-color experiments presented in Supplementary Fig.6b and 8, a carboxyl terminal YFP fusion construct of ScFv5 (referred to as ScFv5-YFP) was transfected instead

of HA tagged ScFv5, and 24h post-transfection, cells were seeded into glass bottom confocal dishes (35 X 10 mm from SPL Lifesciences, South Korea). For the rest of the live cells confocal experiments presented in the manuscript (Fig. 4b-c, Supplementary Fig. 9-11 and 15), cells were transfected with $V_2R$, βarr2-mCherry and HA tagged ScFv5, and the localization of βarr2-mCherry was visualized. For confocal microscopy, we used the Zeiss LSM 710 NLO confocal microscope with oil-immersion 63X /1.40 NA objective housed in a $CO_2$ enclosure with a temperature controlled platform and equipped with 32x array GaAsP descanned detector (Zeiss). We used a Multiline Argon laser for green channel (488 nm), a Diode Pump Solid State Laser for the red channel (561 nm) and a Ti:sapphire laser (Coherent) for DAPI channel. Laser intensity and pinhole settings were kept in the same range for parallel set of experiments and spectral overlap for any two channels was avoided by adjusting proper filter excitation regions and bandwidths. For live cell imaging, time lapsed images were acquired at 30-60 sec intervals and images were finally processed in ZEN lite (ZEN-blue/ZEN-black) software suite from ZEISS. For quantification of receptor endocytosis (Supplementary Fig. 9-12 and 15), images were captured at multiple Z-stacks to cover the entire depth of the cells, and puncta were counted in these different Z-stack images across several fields. Line-scan analysis (Supplementary Fig. 13) was done using ImageJ plot profile plug-in to measure fluorescence intensities across a drawn line. Graphs were plotted after intensities were normalized by subtracting background.

For measuring ligand-induced endocytosis of Tfr1 (Supplementary Fig. 17), HEK-293 cells expressing a recombinant human Tfr1 and ScFv (CTL or 5) were seeded on to poly-D-lysine coated glass-bottom confocal dishes as described above. 48h post-transfection, cells were serum starved (2h), washed with PBS and incubated on ice for 15 min. Subsequently, cells were incubated with DyLight 488-conjugated holo-transferrin (100μg/ml) for 30 min on ice (for ligand binding). Afterwards, cells were washed with ice-cold PBS and then incubated at 37°C for 30 min (to trigger Tfr1 internalization). Subsequently, cells were gently acid-washed (0.1 M glycine, 150 mM NaCl, pH 3) to remove remaining surface-bound holo-transferrin (i.e. non-internalized Tfr1) and then used for imaging. Confocal microscopy on these cells was performed essentially as described above (i.e. ScFv-CTL and ScFv5 cells were imaged under identical imaging conditions) by taking images at multiple Z-positions and analyzed in ZEN lite software suite. Puncta (representing internalized Tfr1) in approximately 100 cells taken from different fields of two independent transfections were counted manually as described above (from images captured at multiple Z-positions). In addition, the mean fluorescence intensity was assessed (as an alternative measure of Trf1 internalization) using the ROI manager plug-in of the ImageJ software in multi measure mode by selecting the entire cytoplasm as region of interest (ROI). Confocal microscopy experiments (CTL vs. ScFv5) were carried out in parallel, under near-identical conditions of transfection and imaging (i.e. transfections in parallel and imaging on the same day with similar microscopy settings). Confocal settings were maintained to near-identical levels even for the experimental replicates carried out on different days.

## FACS (Fluorescence Activated Cell Sorting)

For measuring Tfr1 endocytosis by FACS (Supplementary Fig. 16), HEK-293 cells expressing Tfr1 and ScFv (CTL or 5) were serum starved for 2h, washed with PBS and

subsequently flushed in Tyrode's buffer. Cells were incubated with DyLight 488-conjugated holo-transferrin and washed as described above for confocal microscopy. Finally, the cells were resuspended in Tyrode's buffer containing 1% BSA and used for FACS analysis in a Sysmex Partec CyFlow space Flow Cytometer (Fl-1 channel). Identical acquisition settings were used for all samples in order to allow comparative analysis. Data analysis was performed by FloMax software suite (Partec GmbH, Germany) and the data were interpreted as histograms. Non-transfected cells (without incubation with holo-transferrin) were gated as negative signal to determine real signal form transferrin internalized cells. The relative positive percentage of internalized transferrin cells were calculated relative to the MFI of cells without internalization. Histograms include percentage of positive events (number beyond gate RN1) and levels of mean fluorescence intensity (MFI) of DyLight 488-conjugated transferrin internalization.

### Agonist-induced endocytosis experiments

HEK-293 cells were co-transfected with indicated receptor and ScFv plasmids each in a 10 cm plate. After 24 hrs, $0.15 \times 10^6$ cells were seeded onto a 24 well plate pre-coated with 0.01% Poly-D-lysine (Sigma Aldrich). Cells were serum starved for 2 hrs in serum free media, 48 hrs post transfection. Stimulation was carried out using respective agonists (Genscript/Sigma/ApexBio) (concentrations are mentioned in the figure legends) for indicated time points followed by washing with ice cold 1XTBS twice. Cells were fixed using 4% paraformaldehyde for 20 mins on ice. Blocking was done using 1% BSA prepared in 1X TBS for 2 hrs. This was followed by incubation with anti-FLAG M2 antibody (Sigma, 1:2000 dilution) in TBS+1% BSA (w/v) for 2 hrs at room temperature. Subsequent washes were done with TBS+1% BSA (w/v). For measuring surface expression of receptors at specified time points, cells were incubated with 200 μl of 3,3',5,5'-tetramethylbenzidine (TMB) per well. Reaction was stopped by transferring 100 μl of this colored solution to a 96-well plate already containing 100 μl of 1M $H_2SO_4$. Absorbance was recorded at 450nm in a microplate reader (Victor X4). To account for the total cell density, cells were washed with TBS thrice and then incubated with 200 μl of 0.2% (w/v) Janus green for 10 min. Excess dye was removed by washing the cells with 1 ml of water thrice followed by addition of 800 μl of 0.5M HCL per well. Two hundred microliters of this colored solution was transferred in a 96-well plate and read at 595 nm in a multi-plate reader. The values were normalized by dividing A450 reading with A595 reading.

### ERK MAP kinase assay

HEK-293 cells were co-transfected with indicated receptor and ScFv plasmids. After 24hrs of transfection, $1 \times 10^6$ cells were seeded into a six well plate. Cells were serum starved for 4 hrs in serum free media, 48 hrs post-transfection. Subsequently, cells were stimulated with agonist for indicated time points (concentrations are mentioned in the respective figure legends). Following stimulation, cells were lysed using 2X SDS loading buffer, heated at 95°C for 15 mins and loaded onto 12% SDS-polyacrylamide gel electrophoresis. Subsequently, immunoblotting was performed using PVDF membrane (Biorad). The membrane was blocked using 5% BSA (SRL) for 1h. pERK1/2 were detected by immunoblotting with anti-pERK primary antibody (CST, catalog number 9101, 1:5000 dilution, overnight at 4°C) followed by incubation with anti-rabbit IgG secondary antibody

(Genscript, catalog number A00098, 1:10000) for 1 h. The membrane was washed thrice with 1X TBST and developed using Promega ECL western blotting substrate (catalog number W1001) using a ChemiDoc system (Biorad). pERK1/2 was stripped using 1X stripping buffer and reprobed for tERK1/2 antibody (CST, catalog number 9102, 1:5000 dilution). Blots were quantified by densitometry with Image lab software (5.2.1) and data were analyzed by using GraphPad Prism software.

### Data analysis

Experiments were performed at least three times and data was plotted using GraphPad Prism software. Data was analyzed using appropriate statistical analysis as indicated in figure legends. Details of data normalization are also included in the figure legends.

## Supplementary Material

Refer to Web version on PubMed Central for supplementary material.

## Acknowledgements

The research program in our laboratory is supported by the Indian Institute of Technology Kanpur (IITK/BSBE/2014011), Department of Biotechnology; DBT (BT/08/IYBA/2014/03), Council of Scientific and Industrial Research; CSIR (37(1637)/14/EMR-II), and the Wellcome Trust DBT India Alliance (IA/I/14/1/501285). Dr Shukla is an Intermediate Fellow of the Wellcome Trust/DBT India Alliance (IA/I/14/1/501285). We thankfully acknowledge Linton Traub, Mark Scott, Thomas Pucadyil, Robin Shaw and Roger Davis for the plasmids encoding clathrin terminal domain, βarr2-mCherry, GST-β2 adaptin, hTfr1 (Addgene #69610) and JNK3 (Addgene #15748). We also acknowledge the help from Charu Gupta and Pragya Gupta in the early stages of this work, and Shubhi Pandey for helping in protein purification.

## References

1. Pierce KL, Lefkowitz RJ. Classical and new roles of beta-arrestins in the regulation of G-protein-coupled receptors. Nat Rev Neurosci. 2001; 2:727–733. DOI: 10.1038/35094577 [PubMed: 11584310]
2. DeFea KA. Beta-arrestins as regulators of signal termination and transduction: how do they determine what to scaffold? Cell Signal. 2011; 23:621–629. DOI: 10.1016/j.cellsig.2010.10.004 [PubMed: 20946952]
3. DeWire SM, Ahn S, Lefkowitz RJ, Shenoy SK. Beta-arrestins and cell signaling. Annu Rev Physiol. 2007; 69:483–510. DOI: 10.1146/annurev.ph.69.013107.100021 [PubMed: 17305471]
4. Goodman OB Jr, et al. Beta-arrestin acts as a clathrin adaptor in endocytosis of the beta2-adrenergic receptor. Nature. 1996; 383:447–450. DOI: 10.1038/383447a0 [PubMed: 8837779]
5. Kang DS, Tian X, Benovic JL. Role of beta-arrestins and arrestin domain-containing proteins in G protein-coupled receptor trafficking. Curr Opin Cell Biol. 2014; 27:63–71. DOI: 10.1016/j.ceb.2013.11.005 [PubMed: 24680432]
6. McDonald PH, et al. Beta-arrestin 2: a receptor-regulated MAPK scaffold for the activation of JNK3. Science. 2000; 290:1574–1577. [PubMed: 11090355]
7. Coffa S, et al. The effect of arrestin conformation on the recruitment of c-Raf1, MEK1, and ERK1/2 activation. PLoS One. 2011; 6:e28723.doi: 10.1371/journal.pone.0028723 [PubMed: 22174878]
8. Ahn S, Nelson CD, Garrison TR, Miller WE, Lefkowitz RJ. Desensitization, internalization, and signaling functions of beta-arrestins demonstrated by RNA interference. Proc Natl Acad Sci U S A. 2003; 100:1740–1744. DOI: 10.1073/pnas.262789099 [PubMed: 12582207]
9. Kohout TA, Lin FS, Perry SJ, Conner DA, Lefkowitz RJ. beta-Arrestin 1 and 2 differentially regulate heptahelical receptor signaling and trafficking. Proc Natl Acad Sci U S A. 2001; 98:1601–1606. DOI: 10.1073/pnas.041608198 [PubMed: 11171997]

10. Gurevich VV, Gurevich EV. Structural determinants of arrestin functions. Prog Mol Biol Transl Sci. 2013; 118:57–92. DOI: 10.1016/B978-0-12-394440-5.00003-6 [PubMed: 23764050]
11. Gurevich VV, Gurevich EV. Arrestins: Critical Players in Trafficking of Many GPCRs. Prog Mol Biol Transl Sci. 2015; 132:1–14. DOI: 10.1016/bs.pmbts.2015.02.010 [PubMed: 26055052]
12. Wang Y, et al. Association of beta-arrestin and TRAF6 negatively regulates Toll-like receptor-interleukin 1 receptor signaling. Nat Immunol. 2006; 7:139–147. DOI: 10.1038/ni1294 [PubMed: 16378096]
13. Milano SK, Kim YM, Stefano FP, Benovic JL, Brenner C. Nonvisual arrestin oligomerization and cellular localization are regulated by inositol hexakisphosphate binding. J Biol Chem. 2006; 281:9812–9823. DOI: 10.1074/jbc.M512703200 [PubMed: 16439357]
14. Zhan X, Perez A, Gimenez LE, Vishnivetskiy SA, Gurevich VV. Arrestin-3 binds the MAP kinase JNK3alpha2 via multiple sites on both domains. Cell Signal. 2014; 26:766–776. DOI: 10.1016/j.cellsig.2014.01.001 [PubMed: 24412749]
15. Miller WE, et al. beta-arrestin1 interacts with the catalytic domain of the tyrosine kinase c-SRC. Role of beta-arrestin1-dependent targeting of c-SRC in receptor endocytosis. J Biol Chem. 2000; 275:11312–11319. [PubMed: 10753943]
16. Song X, Gurevich EV, Gurevich VV. Cone arrestin binding to JNK3 and Mdm2: conformational preference and localization of interaction sites. J Neurochem. 2007; 103:1053–1062. DOI: 10.1111/j.1471-4159.2007.04842.x [PubMed: 17680991]
17. Song X, Coffa S, Fu H, Gurevich VV. How does arrestin assemble MAPKs into a signaling complex? J Biol Chem. 2009; 284:685–695. DOI: 10.1074/jbc.M806124200 [PubMed: 19001375]
18. Zhan X, et al. Peptide mini-scaffold facilitates JNK3 activation in cells. Sci Rep. 2016; 6:21025.doi: 10.1038/srep21025 [PubMed: 26868142]
19. Shukla AK, et al. Structure of active beta-arrestin-1 bound to a G-protein-coupled receptor phosphopeptide. Nature. 2013; 497:137–141. DOI: 10.1038/nature12120 [PubMed: 23604254]
20. Xiao K, Shenoy SK, Nobles K, Lefkowitz RJ. Activation-dependent conformational changes in {beta}-arrestin 2. J Biol Chem. 2004; 279:55744–55753. DOI: 10.1074/jbc.M409785200 [PubMed: 15501822]
21. Nobles KN, Guan Z, Xiao K, Oas TG, Lefkowitz RJ. The active conformation of beta-arrestin1: direct evidence for the phosphate sensor in the N-domain and conformational differences in the active states of beta-arrestins1 and -2. J Biol Chem. 2007; 282:21370–21381. DOI: 10.1074/jbc.M611483200 [PubMed: 17513300]
22. Kumari P, et al. Functional competence of a partially engaged GPCR-beta-arrestin complex. Nat Commun. 2016; 7:13416.doi: 10.1038/ncomms13416 [PubMed: 27827372]
23. Zhan X, Gimenez LE, Gurevich VV, Spiller BW. Crystal structure of arrestin-3 reveals the basis of the difference in receptor binding between two non-visual subtypes. J Mol Biol. 2011; 406:467–478. DOI: 10.1016/j.jmb.2010.12.034 [PubMed: 21215759]
24. Hirsch JA, Schubert C, Gurevich VV, Sigler PB. The 2.8 A crystal structure of visual arrestin: a model for arrestin's regulation. Cell. 1999; 97:257–269. [PubMed: 10219246]
25. Srivastava A, Gupta B, Gupta C, Shukla AK. Emerging Functional Divergence of beta-Arrestin Isoforms in GPCR Function. Trends Endocrinol Metab. 2015; 26:628–642. DOI: 10.1016/j.tem.2015.09.001 [PubMed: 26471844]
26. Miller KR, et al. T cell receptor-like recognition of tumor in vivo by synthetic antibody fragment. PLoS One. 2012; 7:e43746.doi: 10.1371/journal.pone.0043746 [PubMed: 22916301]
27. Paduch M, et al. Generating conformation-specific synthetic antibodies to trap proteins in selected functional states. Methods. 2013; 60:3–14. DOI: 10.1016/j.ymeth.2012.12.010 [PubMed: 23280336]
28. Zhong N, et al. Optimizing Production of Antigens and Fabs in the Context of Generating Recombinant Antibodies to Human Proteins. PLoS One. 2015; 10:e0139695.doi: 10.1371/journal.pone.0139695 [PubMed: 26437229]
29. Krupnick JG, Goodman OB Jr, Keen JH, Benovic JL. Arrestin/clathrin interaction. Localization of the clathrin binding domain of nonvisual arrestins to the carboxy terminus. J Biol Chem. 1997; 272:15011–15016. [PubMed: 9169476]

30. Oakley RH, Laporte SA, Holt JA, Caron MG, Barak LS. Differential affinities of visual arrestin, beta arrestin1, and beta arrestin2 for G protein-coupled receptors delineate two major classes of receptors. J Biol Chem. 2000; 275:17201–17210. DOI: 10.1074/jbc.M910348199 [PubMed: 10748214]
31. Ren XR, et al. Different G protein-coupled receptor kinases govern G protein and beta-arrestin-mediated signaling of V2 vasopressin receptor. Proc Natl Acad Sci U S A. 2005; 102:1448–1453. DOI: 10.1073/pnas.0409534102 [PubMed: 15671180]
32. Luo J, Busillo JM, Benovic JL. M3 muscarinic acetylcholine receptor-mediated signaling is regulated by distinct mechanisms. Mol Pharmacol. 2008; 74:338–347. DOI: 10.1124/mol.107.044750 [PubMed: 18388243]
33. Lai X, et al. Agonist-induced activation of histamine H3 receptor signals to extracellular signal-regulated kinases 1 and 2 through PKC-, PLD-, and EGFR-dependent mechanisms. J Neurochem. 2016; 137:200–215. DOI: 10.1111/jnc.13559 [PubMed: 26826667]
34. Daaka Y, et al. Essential role for G protein-coupled receptor endocytosis in the activation of mitogen-activated protein kinase. J Biol Chem. 1998; 273:685–688. [PubMed: 9422717]
35. Wei H, Ahn S, Barnes WG, Lefkowitz RJ. Stable interaction between beta-arrestin 2 and angiotensin type 1A receptor is required for beta-arrestin 2-mediated activation of extracellular signal-regulated kinases 1 and 2. J Biol Chem. 2004; 279:48255–48261. DOI: 10.1074/jbc.M406205200 [PubMed: 15355986]
36. Shenoy SK, et al. Ubiquitination of beta-arrestin links seven-transmembrane receptor endocytosis and ERK activation. J Biol Chem. 2007; 282:29549–29562. DOI: 10.1074/jbc.M700852200 [PubMed: 17666399]
37. Kramer HK, Simon EJ. mu and delta-opioid receptor agonists induce mitogen-activated protein kinase (MAPK) activation in the absence of receptor internalization. Neuropharmacology. 2000; 39:1707–1719. [PubMed: 10884553]
38. Whistler JL, von Zastrow M. Dissociation of functional roles of dynamin in receptor-mediated endocytosis and mitogenic signal transduction. J Biol Chem. 1999; 274:24575–24578. [PubMed: 10455121]
39. DeGraff JL, Gagnon AW, Benovic JL, Orsini MJ. Role of arrestins in endocytosis and signaling of alpha2-adrenergic receptor subtypes. J Biol Chem. 1999; 274:11253–11259. [PubMed: 10196213]
40. Blaukat A, et al. Activation of mitogen-activated protein kinase by the bradykinin B2 receptor is independent of receptor phosphorylation and phosphorylation-triggered internalization. FEBS Lett. 1999; 451:337–341. [PubMed: 10371216]
41. van Koppen CJ, Jakobs KH. Arrestin-independent internalization of G protein-coupled receptors. Mol Pharmacol. 2004; 66:365–367. DOI: 10.1124/mol.104.003822 [PubMed: 15322226]
42. Pals-Rylaarsdam R, et al. Internalization of the m2 muscarinic acetylcholine receptor. Arrestin-independent and -dependent pathways. J Biol Chem. 1997; 272:23682–23689. [PubMed: 9295310]
43. Bowen-Pidgeon D, Innamorati G, Sadeghi HM, Birnbaumer M. Arrestin effects on internalization of vasopressin receptors. Mol Pharmacol. 2001; 59:1395–1401. [PubMed: 11353798]
44. Farrens DL, Altenbach C, Yang K, Hubbell WL, Khorana HG. Requirement of rigid-body motion of transmembrane helices for light activation of rhodopsin. Science. 1996; 274:768–770. [PubMed: 8864113]
45. Kim YM, Benovic JL. Differential roles of arrestin-2 interaction with clathrin and adaptor protein 2 in G protein-coupled receptor trafficking. J Biol Chem. 2002; 277:30760–30768. DOI: 10.1074/jbc.M204528200 [PubMed: 12070169]
46. Breitman M, et al. Silent scaffolds: inhibition OF c-Jun N-terminal kinase 3 activity in cell by dominant-negative arrestin-3 mutant. J Biol Chem. 2012; 287:19653–19664. DOI: 10.1074/jbc.M112.358192 [PubMed: 22523077]
47. Coffa S, Breitman M, Spiller BW, Gurevich VV. A single mutation in arrestin-2 prevents ERK1/2 activation by reducing c-Raf1 binding. Biochemistry. 2011; 50:6951–6958. DOI: 10.1021/bi200745k [PubMed: 21732673]
48. Qian H, Pipolo L, Thomas WG. Association of beta-Arrestin 1 with the type 1A angiotensin II receptor involves phosphorylation of the receptor carboxyl terminus and correlates with receptor

internalization. Mol Endocrinol. 2001; 15:1706–1719. DOI: 10.1210/mend.15.10.0714 [PubMed: 11579203]

49. Malik R, Marchese A. Arrestin-2 interacts with the endosomal sorting complex required for transport machinery to modulate endosomal sorting of CXCR4. Mol Biol Cell. 2010; 21:2529–2541. DOI: 10.1091/mbc.E10-02-0169 [PubMed: 20505072]
50. Alekhina O, Marchese A. beta-Arrestin1 and Signal-transducing Adaptor Molecule 1 (STAM1) Cooperate to Promote Focal Adhesion Kinase Autophosphorylation and Chemotaxis via the Chemokine Receptor CXCR4. J Biol Chem. 2016; 291:26083–26097. DOI: 10.1074/jbc.M116.757138 [PubMed: 27789711]
51. Staus DP, et al. Regulation of beta2-adrenergic receptor function by conformationally selective single-domain intrabodies. Mol Pharmacol. 2014; 85:472–481. DOI: 10.1124/mol.113.089516 [PubMed: 24319111]
52. Shukla AK. Biasing GPCR signaling from inside. Sci Signal. 2014; 7:pe3.doi: 10.1126/scisignal.2005021 [PubMed: 24473194]
53. Carr R 3rd, et al. Development and characterization of pepducins as Gs-biased allosteric agonists. J Biol Chem. 2014; 289:35668–35684. DOI: 10.1074/jbc.M114.618819 [PubMed: 25395624]
54. Quoyer J, et al. Pepducin targeting the C-X-C chemokine receptor type 4 acts as a biased agonist favoring activation of the inhibitory G protein. Proc Natl Acad Sci U S A. 2013; 110:E5088–5097. DOI: 10.1073/pnas.1312515110 [PubMed: 24309376]
55. Beautrait A, et al. A new inhibitor of the beta-arrestin/AP2 endocytic complex reveals interplay between GPCR internalization and signalling. Nat Commun. 2017; 8:15054.doi: 10.1038/ncomms15054 [PubMed: 28416805]
56. Eichel K, Jullie D, von Zastrow M. beta-Arrestin drives MAP kinase signalling from clathrin-coated structures after GPCR dissociation. Nat Cell Biol. 2016; 18:303–310. DOI: 10.1038/ncb3307 [PubMed: 26829388]
57. Ranjan R, Gupta P, Shukla AK. GPCR Signaling: beta-arrestins Kiss and Remember. Curr Biol. 2016; 26:R285–288. DOI: 10.1016/j.cub.2016.02.056 [PubMed: 27046816]



Europe PMC Funders Author Manuscripts

Europe PMC Funders Author Manuscripts

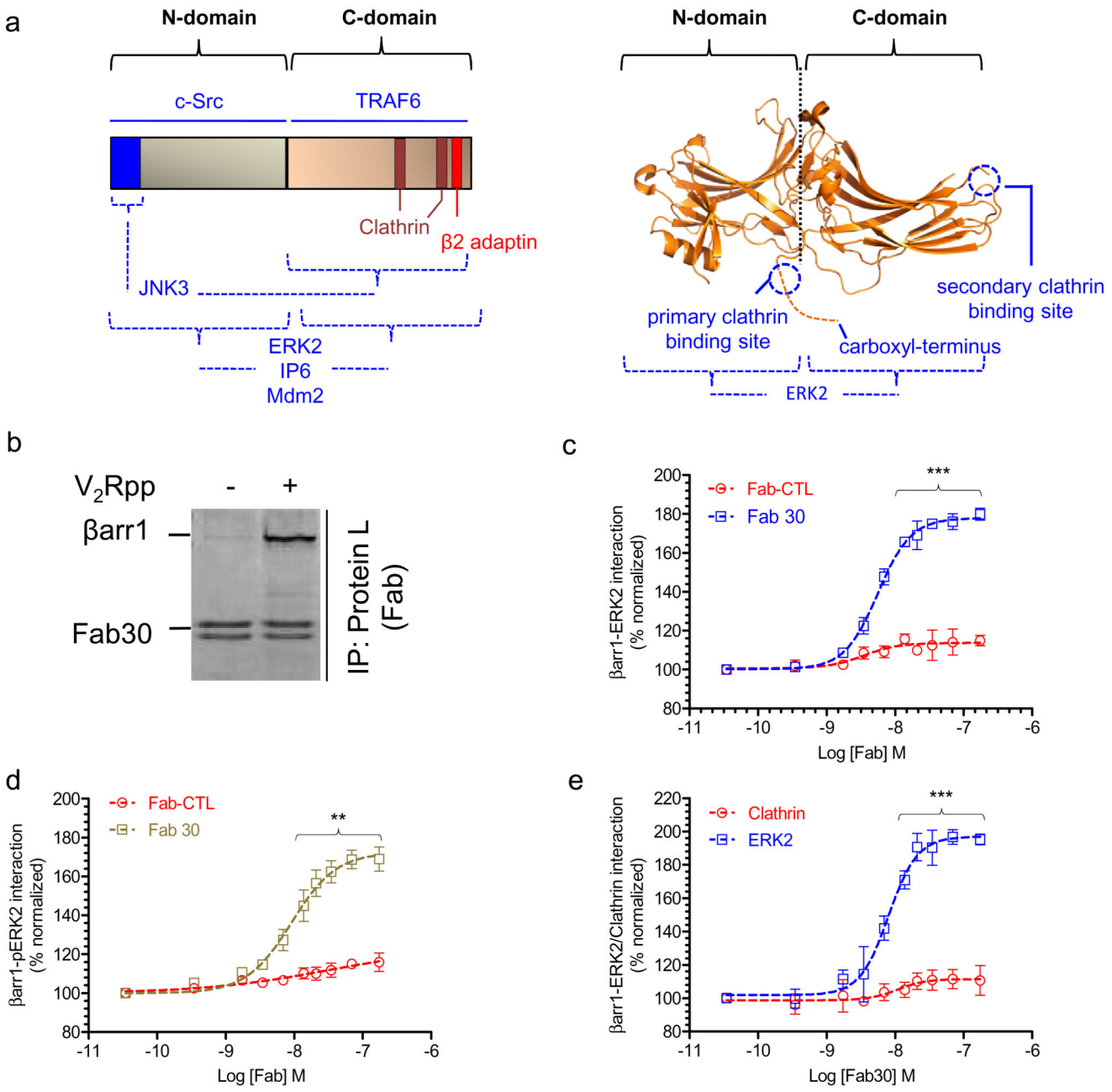


**Figure 1. Allosteric modulation of βarr1-ERK2 interactions by Fab30.**

**a**, Schematic representation of βarr structure showing binding regions for different interaction partners. While clathrin and β2 adaptin have primary binding sites located in the carboxyl terminus of βarrs, JNK3 and ERK2 utilize both, the N- and the C-domain of βarrs. Binding of JNK3 to N-domain primarily requires the residues 1-25. The crystal structure of βarr1-clathrin has revealed a secondary binding site in the C-domain while IP6 has a high-affinity binding site in the C-domain and a low affinity binding site in the N-domain. These binding regions are indicated based on previously published biochemical mapping experiments. The three-dimensional structure shown in the right panel represents the active

βarr1 crystal structure determined previously (PDB ID: 4JQI). **b**, Selectivity of Fab30 for $V_2$Rpp-bound conformation of βarr1 as assessed by a coimmunoprecipitation (coIP) experiment in presence or absence of $V_2$Rpp. The image represents coIP samples resolved by SDS-PAGE and visualized using SimplyBlue staining of the gel. **c**, Effect of Fab30 on the interaction between βarr1 and ERK2 (basal conformation i.e. non-phosphorylated) as assessed by ELISA. Purified ERK2 was immobilized on MaxiSorp ELISA plates and biotinylated βarr1 pre-incubated with varying dosage of either Fab30 or Fab-CTL (negative control) was added to the wells. After rigorous washing, βarr1-ERK2 interaction was detected using HRP-coupled streptavidin. **d**, Effect of Fab30 on the interaction of βarr1 and active ERK2 (phosphorylated) as assessed by ELISA. This experiment was performed in a similar fashion as described in panel c except that *in-vitro* phosphorylated ERK2 (pERK2) was used. **e**, Effect of Fab30 on the interaction of βarr1 with clathrin (terminal domain) and ERK2 as assessed by ELISA. Here, equal concentrations of purified clathrin and ERK2 were immobilized in parallel and their interactions with βarr1 were measured using the same protocol as described in panel c. In the experiments presented in panels c-e, we have used $V_2$Rpp-bound βarr1 as binding of Fab30 to βarr1 requires $V_2$Rpp. (***P*<0.01; ****P*<.001, Two-Way ANOVA; comparison between Fab-CTL and Fab30 or Clathrin and ERK2).

Europe PMC Funders Author Manuscripts

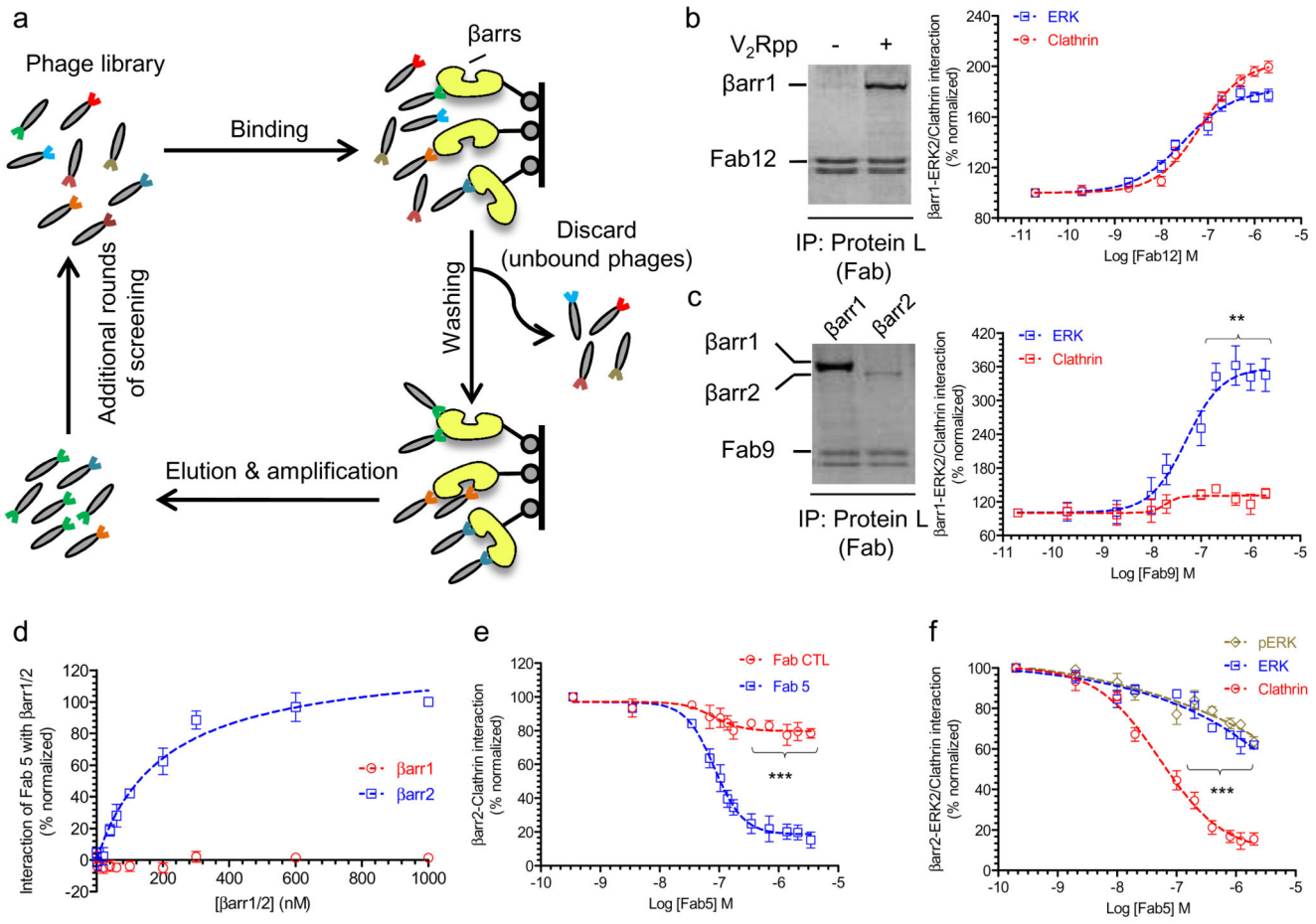


**Figure 2. Selective modulation of βarr-clathrin/ERK2 interactions by βarr-targeting synthetic antibody fragments.**

**a**, Schematic representation of phage display based screening of Fabs against βarrs. Three different βarr targets (βarr1-$V_2$Rpp-Fab30 complex, βarr1 and βarr2) were biotinylated and immobilized on magnetic streptavidin beads. Subsequently, immobilized βarr targets were incubated with a phage display library of antigen binding fragments (Fab) followed by extensive washing and elution of bound phages using DTT. Selected Fab clones were tested for target binding using single point phage ELISA followed by their expression and purification in *E. coli* for detailed characterization. **b**, The ability of Fab12, one of the Fabs selected on βarr1-$V_2$Rpp-Fab30 complex, to selectively recognize $V_2$Rpp-bound βarr1, and its effect on βarr1-ERK2/clathrin interactions in presence of $V_2$Rpp. Similar to Fab30, Fab12 selectively recognized $V_2$Rpp-bound βarr1 conformation as evaluated by coimmunoprecipitation assay. However, unlike Fab30, Fab12 potentiated both, βarr1-ERK2 and βarr1-clathrin interactions. **c**, The ability of Fab9, one of the Fabs selected against βarr1, to selectively recognize βarr1, and its effect on βarr1-ERK2/clathrin interactions in presence of $V_2$Rpp. Fab9 selectively recognizes βarr1 over βarr2, and it selectively potentiated βarr1-ERK2 interaction but not βarr1-clathrin interaction. **d**, Selectivity of Fab5, one of the Fabs selected against βarr2, as measured by ELISA. Indicated concentrations of βarr1/2 were immobilized on ELISA plates followed by incubation with fixed concentration of Fab5.

After rigorous washing, the interaction of Fab5-βarrs was visualized using HRP-coupled Protein L. **e**, Inhibition of βarr2-clathrin interaction by Fab5. Purified clathrin was immobilized on ELISA plates followed by incubation with $V_2$Rpp-bound βarr2 pre-incubated with varying dosage of Fab5 or Fab-CTL. Subsequently, βarr2-clathrin interactions were detected using HRP-coupled streptavidin. Data are normalized with respect to no Fab condition as the reference (treated as 100%). **f**, Selective inhibition of βarr2-clathrin interaction by Fab5. Purified clathrin or ERK2/pERK2 were immobilized on ELISA plates followed by addition of $V_2$Rpp-bound βarr2 pre-incubated with varying dosage of Fab5. Subsequently, the βarr2-clathrin/ERK2/pERK2 interactions were detected using HRP-coupled streptavidin. Data in panels b, c, e and f are normalized with respect to no-Fab pre-incubation condition (i.e. βarr-clathrin/ERK2 interaction without any Fab) as the reference (treated as 100%), and represent an average ± SEM of three independent experiments each carried out in duplicate. Data in panel d is normalized with signal at maximum βarr2 condition (treated as 100%), and represent average ± SEM of three independent experiments each carried out in duplicate. $^{**}P<0.01$; $^{***}P<0.001$, Two-Way ANOVA (comparison between Clathrin and ERK2 or Fab-CTL and Fab5).

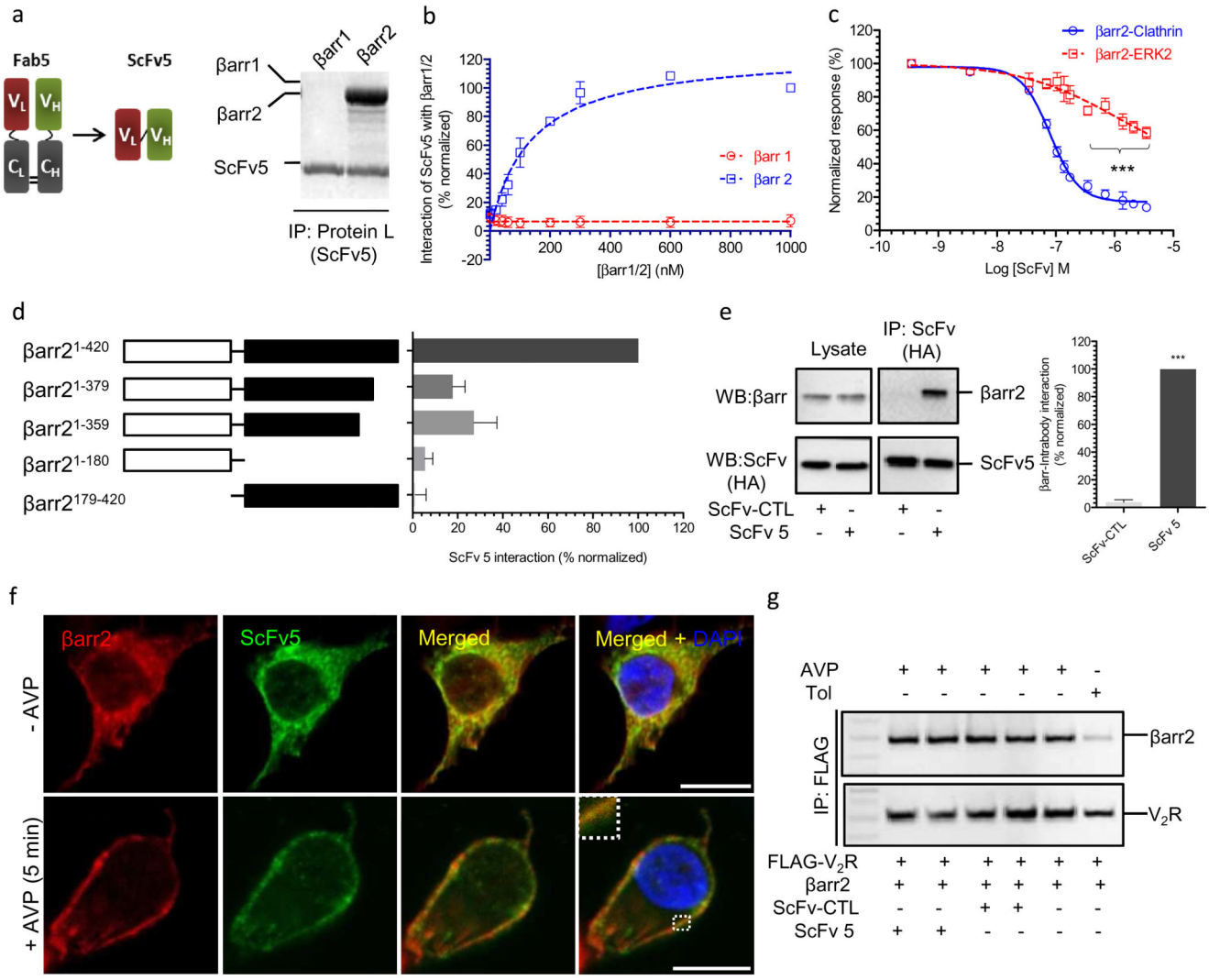


**Figure 3. Characterization of βarr2-ScFv5 interaction and functional validation of ScFv5 intrabody.**

**a**, ScFv version of Fab 5, referred to as ScFv5, maintains selectivity for βarr2 as assessed by a coIP assay. Purified ScFv5 was mixed with equal concentrations of purified βarr1/2 followed by coIP using Protein L beads and detection by Simply Blue staining. **b**, Selective recognition of βarr2 by ScFv5 over βarr1 as assessed by ELISA. The experiment was performed the same way as in panel d of Fig. 2 except that ScFv5 was used instead of Fab5. Data represent two independent experiments each performed in duplicate and normalized as indicated in panel d of Fig. 2. **c**, Similar to Fab5, ScFv5 also selectively inhibits βarr2-clathrin interaction but not βarr2-ERK interaction. This experiment was carried out following the same protocol as described in panel f of Fig. 2. ****P*<0.001, Two-Way ANOVA; comparison between clathrin and ERK2). **d**, ScFv5 requires the carboxyl terminus and the N-domain of βarr2 for binding. Equal concentrations of purified βarr2 truncated proteins (N-terminal GST) as indicated in the figure were incubated with a fixed concentration of ScFv5. The interaction of ScFv5 and truncated βarr2 were measured by




Europe PMC Funders Author Manuscripts

Europe PMC Funders Author Manuscripts

coIP using Protein L beads and normalized with respect to WT βarr2 (i.e. βarr2$^{1-420}$) (treated as 100%). The experiment was performed three times and the data represent average ±SEM. **e**, Functionality of ScFv5 as intrabody measured by its ability to coimmunoprecipitate endogenous βarr2. HEK-293 cells expressing HA-tagged ScFv5 were lysed and used for coIP using HA beads followed by detection using Western blotting. **f**, ScFv5 as an intrabody does not interfere with agonist-induced βarr2 recruitment to the human vasopressin receptor ($V_2R$). HEK-293 cells expressing $V_2R$, βarr2-mCherry and HA-tagged ScFv5 were stimulated with agonist (AVP, 100nM) for 5 min, and the localization of βarr2-mCherry and ScFv5 were assessed by confocal microscopy. ScFv5 was recruited to the membrane and colocalized with βarr2-mCherry. DAPI is used for nuclear staining and the scale bar is 10μm. **g**, Pre-incubation of βarr2 with ScFv5 does not affect its interaction with $V_2R$ as measured by coimmunoprecipitation assay. *Sf*9 cells expressing FLAG-$V_2R$ were stimulated with either Tolvaptan (Tol; inverse agonist) or Vasopressin (AVP; agonist) and βarr2 pre-incubated with ScFv5 or ScFv-CTL was added to the cell lysate. Subsequently, the mixture was cross-linked using DSP and the receptor was immunoprecipitated using FLAG M1 beads. The interaction of $V_2R$-βarr2 was visualized by Western blotting.

Europe PMC Funders Author Manuscripts

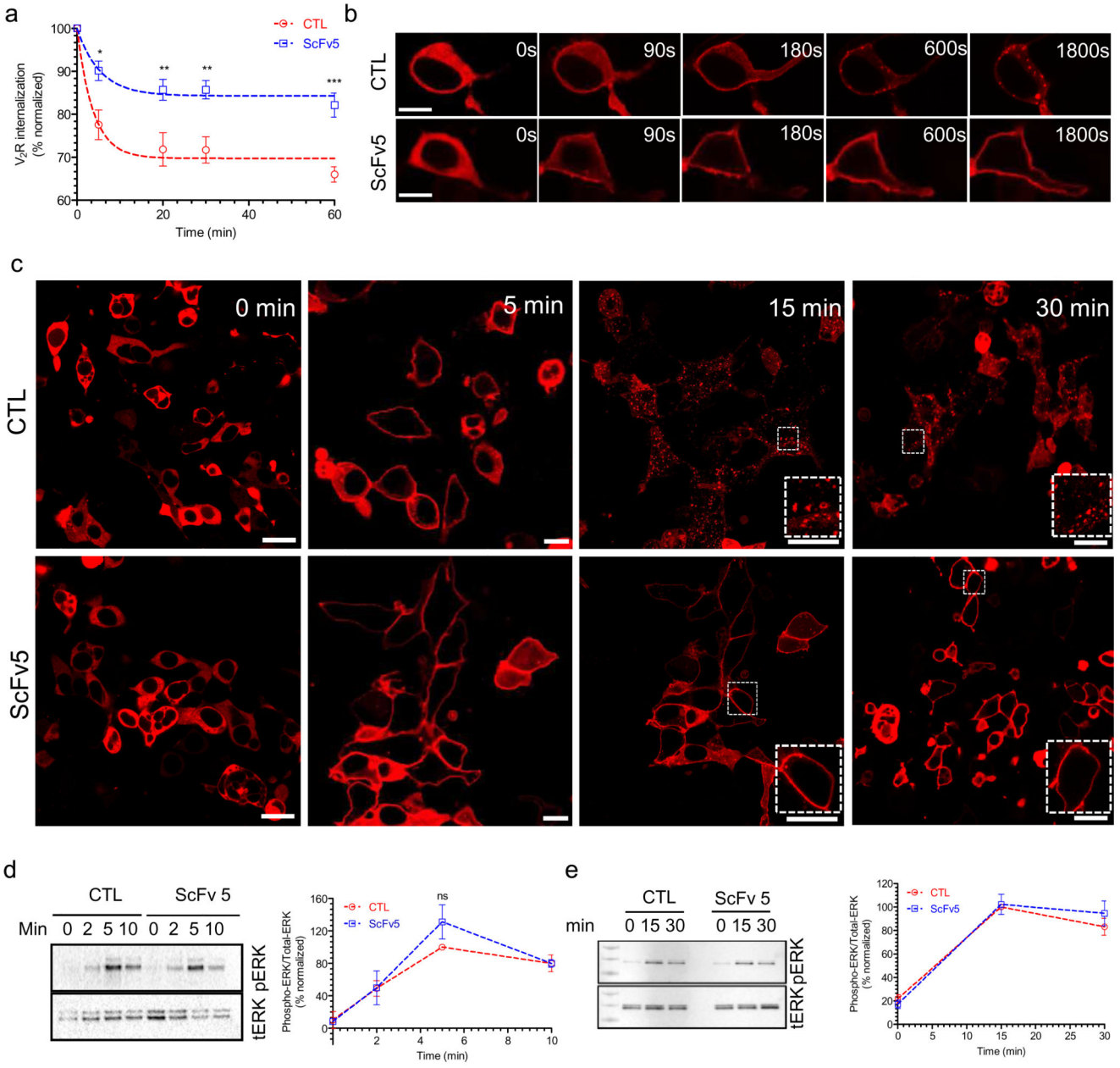


**Figure 4. Selective inhibition of $V_2R$ endocytosis by ScFv5 intrabody.**

**a**, Inhibition of agonist-induced $V_2R$ internalization by ScFv5 intrabody. HEK-293 cells expressing $V_2R$ and either ScFv5 intrabody or a control intrabody were stimulated with 100nM AVP for indicated time points and subsequently used for measuring receptor internalization. Signal intensity at 0 min time point is used as a normalization reference (treated as 100%). Data represents average ± SEM of seven independent experiments each performed in duplicate. *$P$<0.05; **$P$<0.01; ***$P$<0.001, Two-Way ANOVA; comparison between ScFv-CTL and ScFv5. **b** and **c**, Inhibition of agonist-induced $V_2R$ internalization by ScFv5 intrabody assessed by confocal microscopy. HEK-293 cells expressing $V_2R$, βarr2-mCherry and either ScFv5 intrabody or a control intrabody were stimulated with

Europe PMC Funders Author Manuscripts

100nM AVP for indicated time points and subsequently used for confocal microscopy. Cells harboring ScFv5 intrabody displayed membrane localization of βarr2-mcherry even after 30 min post-stimulation suggesting lack of internalization. Control cells on the other hand exhibited robust internalization of $V_2R$ as evident by the accumulation of endocytosis vesicles in the cytoplasm. Scale bar is 10μm. These experiments (CTL vs. ScFv5) were carried out in parallel under near-identical conditions of transfection and imaging. **d**, ScFv5 intrabody does not affect agonist-induced ERK activation downstream of $V_2R$ at both, early and **e**, late time points. HEK-293 cells expressing $V_2R$ and either ScFv5 or ScFv-CTL were stimulated with 100nM AVP for indicated time points and subsequently, cell lysates were used for visualizing ERK phosphorylation. Images in panel d and e are representative of three and seven independent experiments respectively. Graphs show densitometry based quantification of the data normalized with respect to the signal at 5 min (panel d) and 15 min (panel e) in the ScFv-CTL samples (treated as 100%), respectively. ns, non-significant; Two-Way ANOVA.

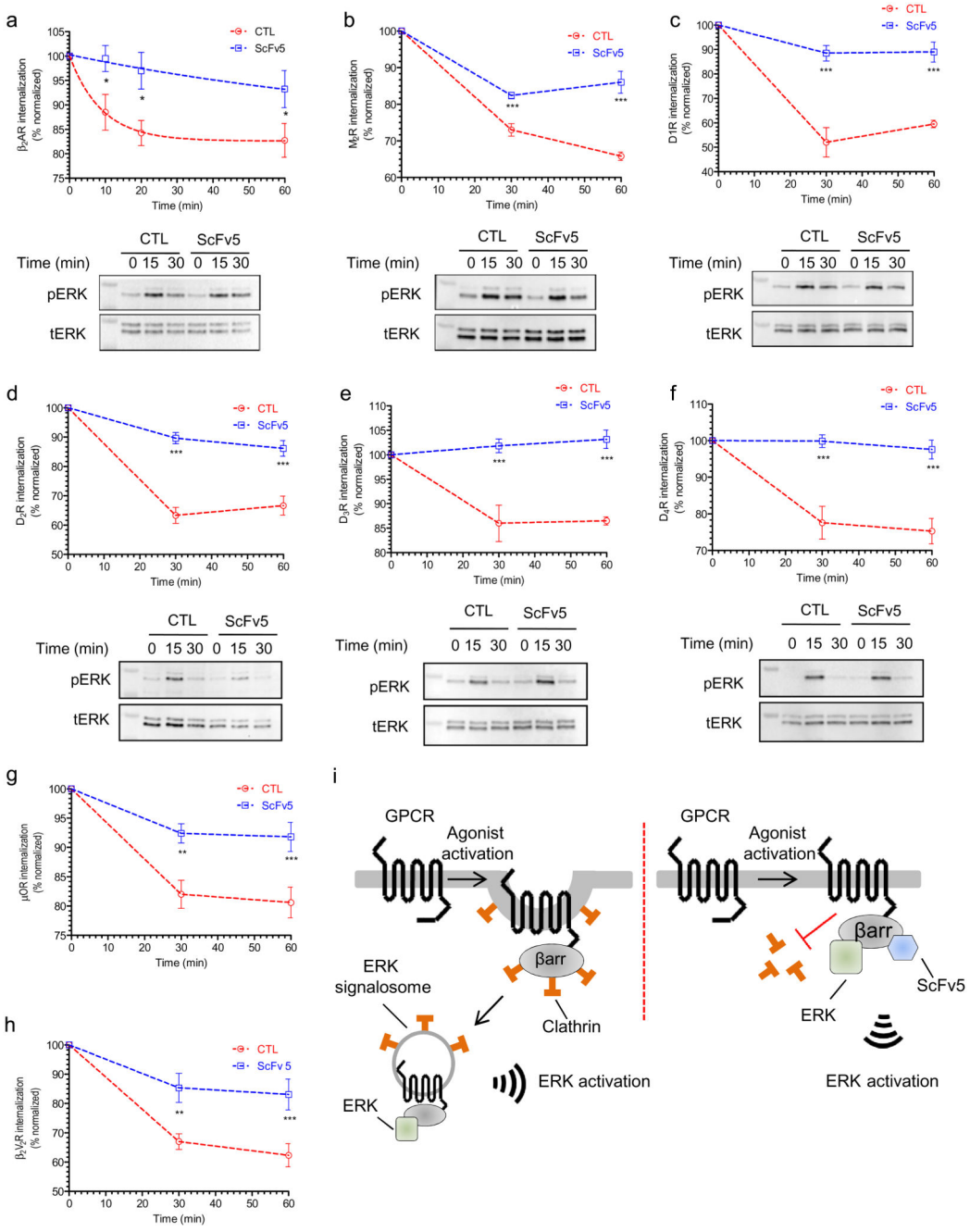


**Figure 5. Generality of ScFv5 as an inhibitor of GPCR endocytosis.**

Inhibition of agonist-induced internalization of **a,** the human β2 adrenergic receptor; $\beta_2$AR, **b,** the human muscarinic receptor subtype 2; $M_2$R, **c,** the human dopamine receptor subtype 1; $D_1$R, **d,** the human dopamine receptor subtype 2; $D_2$R, **e,** the human dopamine receptor subtype 2; $D_3$R, **f,** the human dopamine receptor subtype 4; $D_4$R, **g,** the human μ-opioid receptor; μOR and **h,** a chimeric $\beta_2$AR harboring the carboxyl terminus of $V_2$R, referred to as $\beta_2V_2$R by ScFv5 intrabody. Panels below the internalization plots represent agonist-induced ERK activation from the corresponding receptors. For these experiments, HEK-293

cells were transfected with the indicated receptor and ScFv5 (or a control ScFv) and 48h post-transfection; cells were stimulated with respective agonists for indicated time points to measure receptor internalization (using whole cell ELISA assay) or ERK phosphorylation (Western blotting). For plotting agonist-induced internalization, the signal intensity at 0 min time point is considered 100% and used as a normalization reference. Data represents average ± SEM of 4-7 independent experiments, each performed in duplicate and analyzed using Two-Way ANOVA with Bonferroni post-test (*$P$<0.05; **$P$<.01; ***$P$<0.001). The agonists used here are isoproterenol (10μM for $\beta_2$AR and $\beta_2V_2$R), carbachol (10μM for $M_2$R), dopamine (20μM for $D_1$R, $D_2$R, $D_3$R and $D_4$R), DAMGO (10μM for μOR). **i,** A schematic diagram comparing the notion of ERK signalosome formation as a prerequisite for βarr-dependent ERK activation, and the paradigm presented here suggesting that ERK activation can occur even in the absence of GPCR endocytosis.